



# A unifying Bayesian framework accounting for spatiotemporal interferences with a deceleration tendency

Youguo Chen<sup>a,\*</sup>, Chunhua Peng<sup>b</sup>, Andrew Avitt<sup>c</sup>

<sup>a</sup> Key Laboratory of Cognition and Personality (Ministry of Education), Center of Studies for Psychology and Social Development, Faculty of Psychology, Southwest University, Chongqing 400715, China

<sup>b</sup> Laboratory of Emotion and Mental Health, Chongqing University of Arts and Sciences, Chongqing 402160, China

<sup>c</sup> College of International Studies, Southwest University, Chongqing 400715, China

## ARTICLE INFO

### Keywords:

Bayesian estimation  
Spatiotemporal interference  
Deceleration tendency  
Weber–Fechner law  
Kappa effect

## ABSTRACT

Spatial and temporal levels of information processing interfere with each other. The Kappa effect is a well-known spatiotemporal interference in which the estimated time between two lights increases as the distance between them increases, showing a deceleration tendency. A classical model attributes this interference to constant speeds and predicts a linear relation, whereas a slowness model attributes the interference to slow speeds and proposes that the tendency is due to the uncertainty of stimuli locations. This study integrated a unifying Bayesian framework with the classical model and argued that this tendency is the result of the Weber–Fechner law. This hypothesis was tested via two time discrimination tasks that manipulated the uncertainty of stimuli locations and the distance between stimuli. Experiment 1 showed that the estimated time was not modulated by the uncertainty of the stimuli locations. Experiment 2 revealed that the behavioral predictions made by the Bayesian model on logarithmic scales were more accurate than those made by the linear model. Our results suggest that the deceleration tendency in the Kappa effect is the result of the Weber–Fechner law.

## 1. Introduction

Many tasks require the precise perception of temporal and spatial information. For example, pilots must land the plane in the right place at the right time. The interaction of spatial and temporal representations in the brain has long attracted attention in the fields of psychology and neuroscience (Oliveri et al., 2009). Spatiotemporal interference offers a window by which to investigate the nature of representations of time and space (Casasanto and Boroditsky, 2008; Walsh, 2003). The Kappa effect is one of the most well-known spatiotemporal interferences (Cohen et al., 1953). In the simplest experiment regarding this effect, two lights were flashed in sequence to define the distance and time interval; the perceived time interval seemed to increase as the spatial distance between the two lights increased (Price-Williams, 1954).

Theoretical models have attempted to explain spatiotemporal interference quantitatively. The classical model of the Kappa effect assumes that observers tend to impute motion to the static lights implicitly; the model indicates that the imputed motion has a constant speed (Cohen et al., 1955; Collyer, 1976; Masuda et al., 2011; Price-Williams, 1954). The model quantitatively accounts for the Kappa effect, in which the

perceived inter-stimulus time is a weighted average of the actual time and the expected time, and the expected time is calculated as the ratio of the known distance to a constant speed (Huang and Jones, 1982; Jones and Huang, 1982). A slowness model was proposed to explain the cutaneous rabbit illusion, tactile Kappa effect, tactile temporal order judgment, and spatial attention effects (Goldreich, 2007; Goldreich and Tong, 2013). This model was developed based on the “slow speed prior” hypothesis. The term “slow speed prior” comes from the statistical structure of motion, in which objects tend to be stationary or move slowly (Freeman et al., 2010; Stocker and Simoncelli, 2006; Weiss et al., 2002). The slowness model combines a slow speed prior with tactile spatiotemporal information to obtain an optimal spatiotemporal perception using Bayes’ rule (Goldreich, 2007; Goldreich and Tong, 2013).

Recently, a study demonstrated that the classical model can be rewritten as a Bayesian model with an appropriate definition (Chen et al., 2016). In this study, two circles flashed from the left to the right visual field in sequence. The time interval and the distance between the two circles were manipulated. The subjects were required to reproduce the time interval between the two circles. The study found that the

\* Corresponding author.

E-mail address: [ygchen246@gmail.com](mailto:ygchen246@gmail.com) (Y. Chen).

<https://doi.org/10.1016/j.visres.2021.06.005>

Received 6 January 2021; Received in revised form 13 June 2021; Accepted 13 June 2021

Available online 1 July 2021

0042-6989/© 2021 Elsevier Ltd. All rights reserved.

classical model and the slowness model both replicated the Kappa effect but that the nonlinear slowness model fitted the deceleration tendency better than the linear classical model (i.e., the estimated time increased more slowly with longer distances than it did with shorter distances). However, Chen et al. (2016) pointed out that the slowness model has three disadvantages. First, it has a complex expression, and the estimated time cannot be written as a function of the sample time. Second, the spatial uncertainty of the slowness model, inferred from previous studies, remains unchanged for different participants, but individual differences, luminance contrast, and the shapes of visual stimuli may modulate spatial uncertainty. Finally, the uncertainty of temporal information changes along with the sample time, which prevents the model from predicting the production time for a new sample time. Furthermore, the slowness model attributes the deceleration tendency to the spatial uncertainty of stimuli locations (see “slowness model” in the supplementary materials for details; Chen et al., 2016; Goldreich, 2007); however, the hypothesis that the deceleration tendency is driven by spatial uncertainty has never been tested.

A unifying Bayesian framework has been proposed for estimations of magnitudes, such as loudness, distance, or time. The framework incorporates Weber–Fechner’s law of magnitude estimation with the influence of prior experience; provides a unifying perspective that explains biases in magnitude estimation, such as the regression effect, range effect, scalar variability, and sequential effect; reconciles and provides a re-interpretation of the work of Weber–Fechner and Stevens; and guides future investigations into the neurobiological underpinnings of magnitude estimation for health and psychiatric diseases (Petzschner et al., 2015). Fechner (1860) proposed a logarithmic relationship between physical magnitudes and representations via sensory systems based on Weber’s law. Research findings confirm that magnitude estimations are on a logarithmic scale, such as distance reproduction (Durgin et al., 2009; Lakshminarasimhan et al., 2018; Petzschner and Glasauer, 2011), numerical quantities (Dehaene, 2003; Dehaene et al., 2008), visual motion perception (Stocker and Simoncelli, 2006), and time perception (Brannon et al., 2008; Gibbon, 1977; Gibbon and Church, 1981). As Fechner’s law shows a typical deceleration tendency whereby the subjective sensation is proportional to the logarithm of the stimulus intensity, we postulated that the deceleration tendency in the Kappa effect may be the result of the Weber–Fechner law.

We incorporated the classical model into the Weber–Fechner law according to the unifying Bayesian framework (Petzschner et al., 2015).

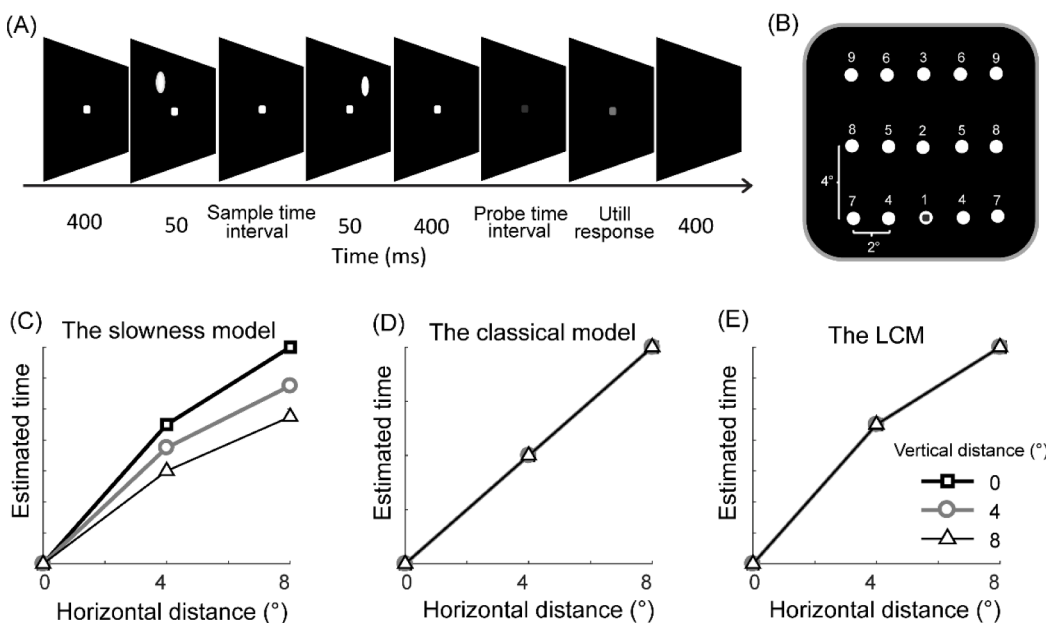


**Fig. 1.** The procedure, stimuli, and predictions of models in Experiment 1. (A) Time discrimination task. The sample was the time interval between two white circles, and the probe was the time interval during the presentation of the blue square. (B) The display positions of circles in Experiment 1. Nine digits represent nine treatments (3 horizontal distances  $\times$  3 vertical distances). The fixation square was presented overlapping with position 1. (C) The slowness model predicts that the estimated time will decrease as the vertical distance increases. (D) The classical model and (E) the LCM predict no effect of the vertical distance on the estimated time.

The logarithmic version of the classical model (LCM) assumes a logarithmic time representation, which is based on the finding that time discrimination approximately follows the Weber–Fechner law (Brannon et al., 2008; Gibbon, 1977; Gibbon and Church, 1981). The physical time and expected time are logarithmically transformed into internal time (Petzschner et al., 2015; Petzschner and Glasauer, 2011; Stocker and Simoncelli, 2006). The estimated internal time is a weighted average internal time as transformed from physical and expected time; this is similar to the classical model, in which the estimated time is a weighted average of physical time and expected time (see supplementary materials for details). We conducted two experiments to investigate whether the deceleration tendency is driven by spatial uncertainty or the Weber–Fechner law. Experiment 1 tested whether the spatial uncertainty of stimuli locations modulated the estimated time (see Fig. 1). Experiment 2, a continuation of Experiment 1, examined whether the deceleration tendency was driven by the Weber–Fechner law (see Fig. 3).

## 2. Experiment 1

The slowness model attributes the deceleration tendency to the spatial uncertainty of stimuli locations (see supplementary materials for details; Chen et al., 2016; Goldreich, 2007). In the test examining whether the spatial uncertainty of stimuli locations modulated time perception, two sample circles flashed from the left to the right visual fields in sequence at nine locations (see Fig. 1A). The horizontal distance between the two circles and the vertical distance between the circles and the central square were randomly chosen from three distances (see Fig. 1B). The classical model, LCM, and slowness model all predict that the estimated time increases as the horizontal distance increases (see Fig. 1C, D, and E; see supplementary materials for details). The slowness model infers that a larger spatial uncertainty results in a greater underestimation of physical distance (Tong et al., 2016) and that a shorter distance produces a shorter duration perception (Chen et al., 2016; Goldreich, 2007). Because the spatial uncertainty of the circle locations increases as vertical distance increases (Levi et al., 1988; Waugh & Levi, 1993), the slowness model predicts that the estimated time will decrease as the vertical distance increases (see Fig. 1C). Given a horizontal distance, two circles always appear in the same row; thus, the straight-line distance between two circles is the same for different vertical distances (see Fig. 1B). Furthermore, the classical model and the LCM are

unrelated to the spatial uncertainty of the circle locations; thus, the two models predict that the estimated time will remain constant as vertical distance increases (see Fig. 1D and E).

2.1. Methods

2.1.1. Participants

Twenty participants (11 males, 18–27 years of age) participated in Experiment 1. All participants had normal or corrected-to-normal visual acuity. Informed written consent was obtained from all participants. The study was carried out in accordance with the Declaration of Helsinki (World Medical Association, 2013) and was approved by the Ethics Committee of Southwest University.

2.1.2. Stimuli and procedures

The visual stimuli were displayed on a computer screen with a black background. The screen was a 27-inch and 60 Hz refresh rate. White, blue, or cyan squares were 2 mm in size ( $0.2^\circ$ ). The white circle was 6 mm in diameter ( $0.6^\circ$ ). Stimulus presentation was controlled using MATLAB (MathWorks, Inc., Natick, Massachusetts, USA) and Psychtoolbox 3 (Brainard, 1997). Experiment 1 was modified from a time reproduction task used in Chen et al. (2016). We used a time discrimination task with the constant stimuli method to avoid response bias in the time reproduction task (Chen et al., 2016; Pöppel, 1997; Szelag et al., 2002; Ulbrich et al., 2007).

The participants were seated approximately 60 cm in front of a computer monitor. At the beginning of each trial, a white square appeared in the center of the screen for 0.4 s. The participants were required to fixate on the central square throughout the trial (see Fig. 1A). Two sample circles flashed from the left to the right visual fields in sequence, and then the central square turned blue (the probe). The

horizontal distance between the two circles and the vertical distance between the circles and the central square were randomly chosen from three distances ( $0^\circ$ ,  $4^\circ$ , or  $8^\circ$ ). Circle positions were marked by digits from 1 to 9 for nine treatments ( $3 \times 3$ ; see Fig. 1B). The sample interval between the two circles was 0.5 s. The probe time interval during the presentation of the blue square was randomly chosen from seven durations (0.2, 0.3, 0.4, 0.5, 0.6, 0.7, or 0.8 s). The circles were presented in advance of the blue square in half of the trials, and the blue square was presented in advance in the other half of the trials. Finally, the central square turned cyan as a response signal. We used a two-alternative forced-choice (2-AFC) experimental protocol, in which the participants were asked to select whether the probe time interval of the blue square was shorter or longer than the sample time interval between the two circles. The participants pressed “F” or “J” on the keyboard using the index fingers of both hands (“F” denoted shorter and “J” longer). An inter-trial interval of 0.4 s was used.

We used three horizontal distances, three vertical distances, and seven probe time intervals, and each treatment consisted of 20 trials, with a total of 1260 trials ( $3 \times 3 \times 7 \times 20$ ) in Experiment 1. Participants had a short break (approximately a minute) once they completed 126 trials.

2.1.3. Statistical analysis

Data were fitted by cumulative Gaussians for each condition (see Fig. 2A, B, and C), and the point of subjective equality (PSE) and standard deviation (SD) were calculated using the best-fitting function (Burr et al., 2007, 2009). A two-way repeated-measures analysis of variance (ANOVA) was conducted on the PSE and SD for all participants in Experiment 1. The ANOVA factors were horizontal distance ( $0^\circ$ ,  $4^\circ$ ,  $8^\circ$ ) and vertical distance ( $0^\circ$ ,  $4^\circ$ ,  $8^\circ$ ). The Greenhouse–Geisser correction was used to correct for any violations of sphericity (Greenhouse and

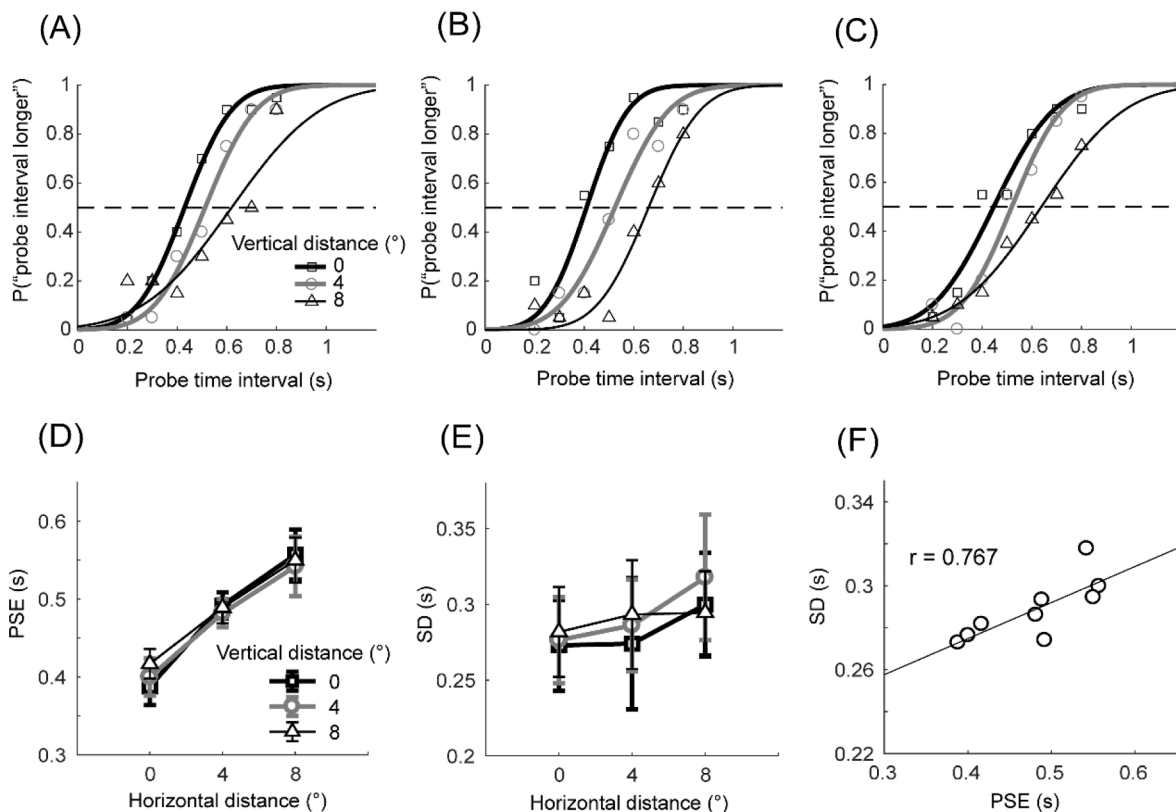


Fig. 2. Behavioral responses for Experiment 1. Responses and corresponding psychometric curves of a representative participant for the (A)  $0^\circ$ , (B)  $4^\circ$ , and (C)  $8^\circ$  vertical distances. (D) Mean point of subjective equality (PSE) and (E) mean standard deviation (SD) of all participants. The error bars indicate one standard error of the mean across all participants. (F) The correlation between mean PSE and mean SD. Nine circles indicate nine treatments ( $3$  horizontal distances  $\times$   $3$  vertical distances).

Geisser, 1959), and the partial eta squared ( $\eta_p^2$ ) was used to estimate the ANOVA effect size (Levine and Hullett, 2002).

## 2.2. Results and discussion

Two circles were presented in sequence at nine locations in Experiment 1 (see Fig. 1). The PSE was estimated for nine stimuli locations (three horizontal distances  $\times$  three vertical distances). For a representative observer, the psychometric curves of the data moved from left to right as the horizontal distance between the two circles increased for vertical distances of 0° (see Fig. 2A), 4° (see Fig. 2B), and 8° (see Fig. 2C). The PSE increased as the horizontal distance increased, whereas the PSE remained constant as the vertical distance increased at the group level (see Fig. 2D).

A two-way repeated-measures ANOVA conducted on the PSE revealed a significant main effect of horizontal distance [ $F(2, 38) = 14.663, p < 0.01, \eta_p^2 = 0.436$ ]. The PSE was significantly smaller in the 0° (mean  $\pm$  SEM:  $0.402 \pm 0.020$  s) than in the 4° ( $0.487 \pm 0.016$  s) and the 8° ( $0.550 \pm 0.032$  s) conditions ( $p < 0.05$ ), and the PSE was significantly smaller in the 4° condition than in the 8° condition ( $p < 0.05$ ). These results replicated the typical Kappa effect, in which the estimated time increased along with the space distance between the circles. The main effects of vertical distance [ $F(2, 38) = 0.617, p > 0.05, \eta_p^2 = 0.031$ ] and the interaction between horizontal and vertical distances [ $F(4, 76) = 0.714, p > 0.05, \eta_p^2 = 0.036$ ] were not significant. The mean PSEs were  $0.479 \pm 0.016$  s,  $0.475 \pm 0.020$  s, and  $0.485 \pm 0.018$  s for 0°, 4°, and 8° vertical distances, which were not consistent with the prediction of the slowness model that time would decrease as the vertical distances increased.

We also conducted statistical power analyses for the main effect of vertical distance using R software with pwr (<https://CRAN.R-project.org/package=pwr>). According to the equation, the effect size  $f$  was 0.179. We can compute the ideal sample size as 101 (Cohen, 1988) given that the ideal statistical power for any study is considered to be 0.8 (Malone et al., 2016), and the significance level is 0.05. A sample size of  $>100$  indicated that the effect of vertical distance on the estimated time was quite weak. In summary, the results indicated that the variance of stimuli locations was not an influencing factor for the Kappa effect.

A two-way repeated-measures ANOVA conducted on the SD showed that the main effects of horizontal distance [ $F(2, 38) = 1.572, p > 0.05, \eta_p^2 = 0.076$ ] and vertical distance [ $F(2, 38) = 0.269, p > 0.05, \eta_p^2 = 0.014$ ] and horizontal distance  $\times$  vertical distance interaction [ $F(4, 76) = 0.315, p > 0.05, \eta_p^2 = 0.016$ ] were not significant. The mean SD increased as the horizontal distance increased ( $0.277 \pm 0.0270$  s,  $0.284 \pm 0.033$  s, and  $0.308 \pm 0.032$  s for 0°, 4°, and 8°). Statistical power analysis was conducted on the main effect of the horizontal distance. The statistical power was 0.8, and the significance level was 0.05. We computed the ideal sample size to be 40, which indicates that the effect of horizontal distance on the SD can be significant if the sample size is increased by a reasonable rate.

The Pearson correlation coefficient was calculated to assess the relationship between the PSE and SD. We found a significantly positive correlation between mean PSE and mean SD ( $r = 0.767, p < 0.05$ ; see Fig. 2F). The result indicating that SD increased with PSE was consistent with the scalar variability whereby the standard deviation of an internal time increases linearly with its mean (Brannon et al., 2008; Gibbon, 1977; Gibbon et al., 1984; Wearden, 1999).

One crucial assumption of this study is that the spatial uncertainty of the circle locations increases as vertical distance increases. This assumption is based on the finding that the spatial uncertainty increases with the increase of the eccentricity (Levi et al., 1988; Waugh & Levi, 1993), and the eccentricity increases as the vertical distance increases (Fig. 1B). The increase in spatial uncertainty with eccentricity has been suggested to arise from a decrease in the precision of retino-cortical mapping (Klein & Levi, 1987; Levi & Klein, 1990), and from increases in the spatial irregularity of the retinal mosaic (Wilson, 1991). Thus the

assumption that vertical displacements increase spatial uncertainty is reasonable.

## 3. Experiment 2

The distance between the two sample circles was randomly chosen from 1° to 32° in Experiment 2, enabling the use of psychophysical functions to assess the fit of the models for the deceleration tendency. The findings showed that the LCM replicated the tendency, rather than the classical model, providing evidence that the deceleration tendency is driven by the Weber–Fechner law.

### 3.1. Methods

#### 3.1.1. Participants

Ten participants (three males, 20–29 years of age) participated in Experiment 2. Other details were the same as those in Experiment 1.

#### 3.1.2. Stimuli and procedures

Experiment 2 (see Fig. 3) used a time discrimination task with the staircase procedure to save time, rather than the constant stimuli method (Meese, 1995). Two sample circles flashed from the left to the right visual fields in sequence. The vertical distance between the circles and the central square was 2.9° (30 mm; Chen et al., 2016). The horizontal distance between the circles was randomly chosen from six distances (1°, 2°, 4°, 8°, 16°, or 32°). Sample time intervals between two sample circles were randomly chosen from two durations (0.5 or 1 s). Then, two probe circles flashed from the left to the right visual fields in sequence. The horizontal distance between the two probe circles was 1°. Probe time intervals between the two probe circles were adjusted according to the interleaved adaptive staircase procedure. One staircase started from 0.4 time of the sample time interval (e.g., 0.2 s for the sample time interval of 0.5 s), and the other staircase started from 1.6 time of the sample time interval. The staircase procedure consisted of the simple up-down method (one up, one down) with a step size of 0.1 time of the sample time interval. The sample circles were presented in advance of the probe circles in half of the trials, and the probe circles were presented in advance in the other half of the trials. Participants were asked to select whether the time interval between the first pair of circles was shorter or longer than that between the second pair. Participants pressed “F” or “J” on the keyboard using the index fingers of both hands (“F” denoted longer and “J” shorter).

The experiment used two sample time intervals and six horizontal distances. Each treatment consisted of two staircases, with 40 trials in each staircase. The 80 trials determined a psychometric function for treatment (Stocker and Simoncelli, 2006). All staircases were randomly interleaved. There were 960 trials ( $2 \times 6 \times 2 \times 40$ ) in Experiment 2. Participants were permitted a short break (of approximately one minute) once they completed 96 trials.

#### 3.1.3. Fitting the models to the data

We first obtained PSE by fitting the cumulative Gaussian function to the data for each treatment and each participant (see Fig. 4A).

Then, the maximum-likelihood estimation was used to estimate the best-fitting parameters of the classical model and the LCM (see Fig. 3B and C; see supplementary materials for details). Observers estimated the probe time interval to be shorter ( $r_i = -1$ ) or longer ( $r_i = +1$ ) than a sample time interval in the  $i$ th trial. Following the signal detection theory (Freeman et al., 2010; Wickens, 2001), the  $d'$  value was calculated for the response in the  $i$ th trial with Equation S5 for the classical model or with Equation S18 for the LCM (see the supplementary materials for details). The probability was calculated using the cumulative standard normal distribution function  $\Phi$ :

$$p(r_i = 1|\theta) = \Phi\left(\frac{d'}{\sqrt{2}}\right), \text{ or } p(r_i = -1|\theta) = 1 - \Phi\left(\frac{d'}{\sqrt{2}}\right) \quad (1)$$

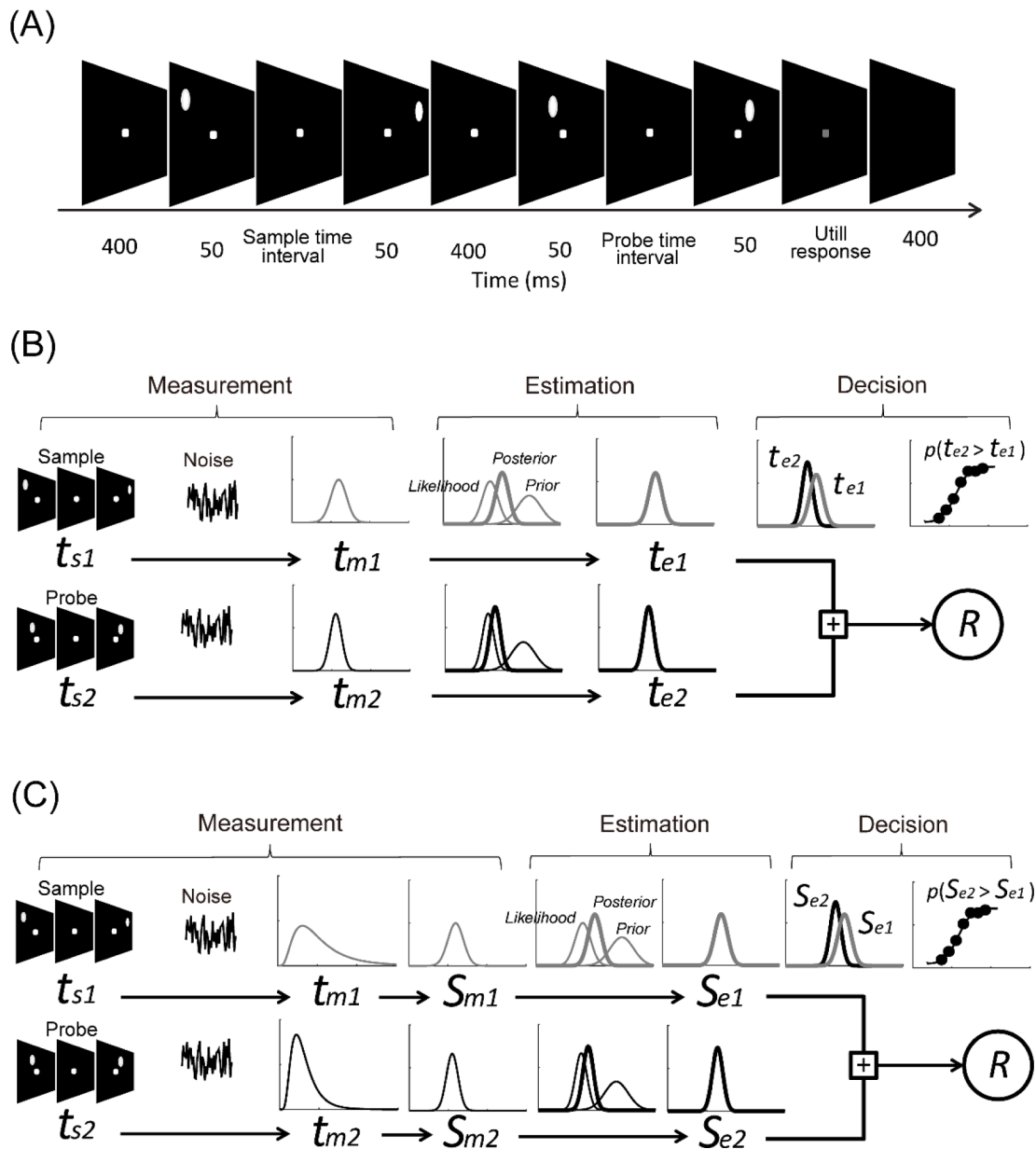


**Fig. 3.** The procedure and Bayesian models in Experiment 2. (A) The procedure of Experiment 2. The sample and probe were the time intervals between two pairs of circles. (B) The classical model for time discrimination task. In each trial, the observer independently performs an optimal time estimation on sample and probe time intervals and then selects the longer estimate in the decision stage. The measured time  $t_m$  is assumed as a normal likelihood function. The responses are modeled using standard methods from signal detection theory. (C) The logarithmic version of the classical model (LCM) for the time discrimination task. The measured time  $t_m$  and expected time  $E(t)$  are assumed as log-normal likelihood functions, and the measured time and expected time are then logarithmically transformed into internal measured time (likelihood,  $S_m$ ) and internal expected time (prior,  $S_e$ ). The internal measured time (likelihood) and the internal expected time (prior) are both normal distributions; thus, the estimation and decision stages of the CLM are similar to those of the classical model.

The responses were assumed to be independent across trials. The joint conditional probability of the responses across all  $n$  trials can be expressed as follows:

$$\log p(r_1, r_2, \dots, r_n | \theta) = \sum_{i=1}^n \log p(r_i | \theta) \quad (2)$$

Parameters  $\theta$  were  $\omega$ ,  $v_0$ , and  $w_m$  for the classical model and  $\omega_s$ ,  $\sigma_{sm}$ ,  $v_0$ , and  $t_0$  for the LCM. The parameters were determined for each participant by maximizing the likelihood using the “fminsearch” command in MATLAB (Freeman et al., 2010). The bootstrap method was used to estimate the standard errors of the parameters for each individual participant (see Supplementary Table 1). We resampled the data with replacement and repeated this resampling 100 times (Chang and Jazayeri, 2018; Jogan and Stocker, 2015; Stocker and Simoncelli, 2006).

The Akaike information criterion (AIC) was used to evaluate the goodness of the model fit. The AIC accounts for overfitting by penalizing models with a greater number of parameters (Akaike, 1974). It is calculated as follows:  $AIC = 2[k - \sum_{i=1}^n \log p(r_i | \theta)]$ , where  $k$  is the number of parameters, and  $\theta$  is the best-fitting parameter of the model. In this study,  $k$  was 3 for the classical model ( $\omega$ ,  $v_0$ ,  $w_m$ ) and 4 for the LCM ( $\omega_s$ ,  $\sigma_{sm}$ ,  $v_0$ ,  $t_0$ ). The AIC difference ( $\Delta$ ) was obtained by subtracting the AIC of the LCM from that of the classical model.

### 3.2. Results and discussion

Experiment 2 supports the assertion that the Weber–Fechner law is critical for the deceleration tendency in the Kappa effect. A 2-FAC time

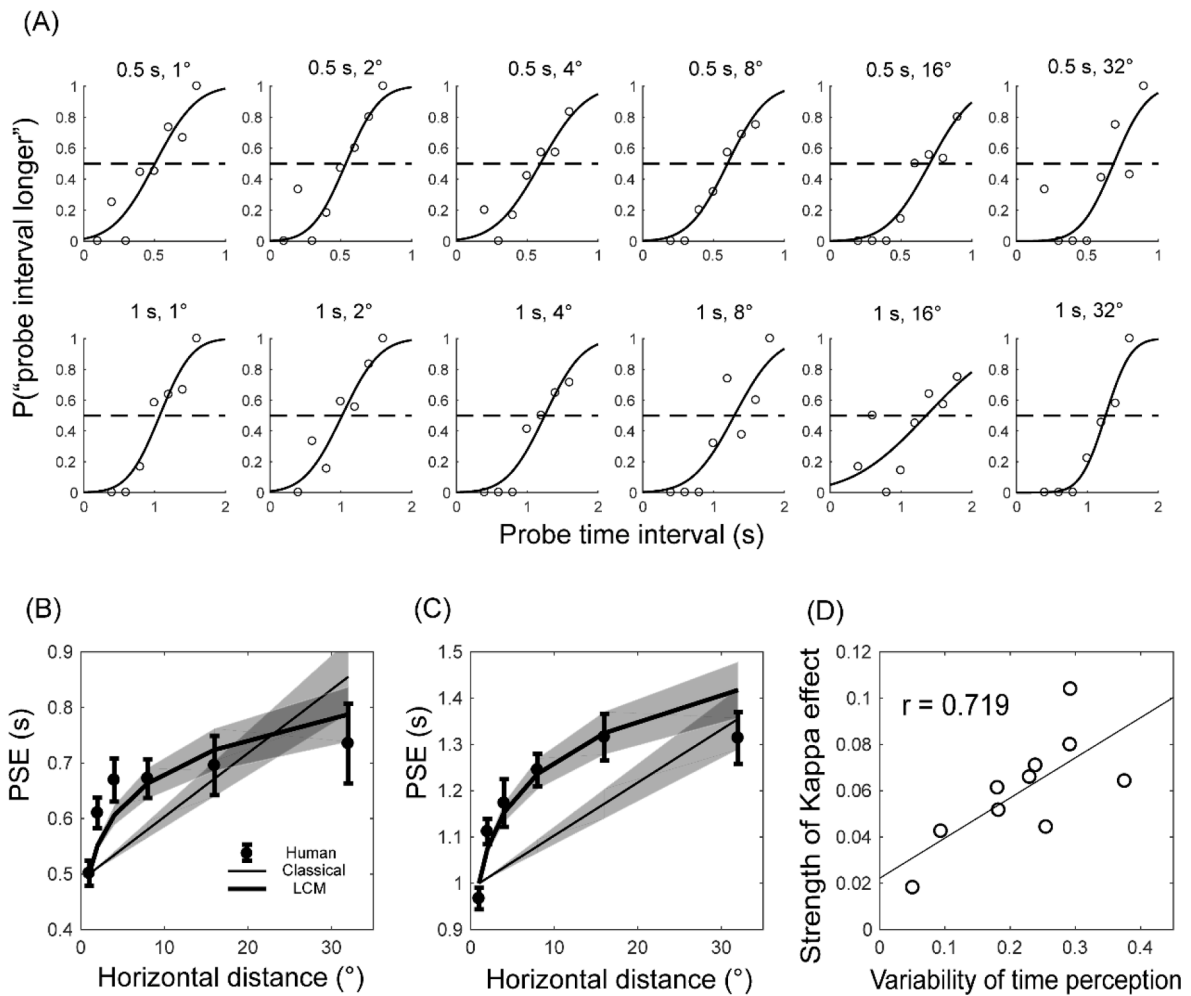


**Fig. 4.** Behavior responses and model fitting for Experiment 2. (A) Responses and corresponding psychometric curves of a representative participant. Mean PSE of all participants and predictions of Bayesian models in the (B) 0.5-second and (C) 1-second conditions. The error bars and shadows indicate one standard error of the mean across all participants. (D) The correlation between variability of time perception ( $\sigma_{sm}$ ) and the strength of the Kappa effect ( $\kappa = 1 - \omega_s$ ). Ten circles indicate 10 participants.

discrimination task was used to characterize the estimated time as a function of the sample time intervals (0.5 and 1 s) and the horizontal distances between the two circles (1°, 2°, 4°, 8°, 16°, 32°; see Fig. 3A). We then fitted the classical model and the LCM to the data to ascertain which model best explained the data.

The PSE was estimated for 12 treatments (two sample time intervals  $\times$  six horizontal distances) for each participant. For a representative observer, the psychometric curves of the data moved from left to right as the horizontal distance between the two circles increased (see Fig. 4A). The deceleration tendency was observed both in the 0.5-second (see Fig. 4B) and 1-second (see Fig. 4C) conditions at the group level.

The LCM seemed to qualitatively explain the human data better than the classical model in both the 0.5-second (see Fig. 4B) and 1-second (see Fig. 4C) conditions. The classical model predicts the PSE as a linear function of the horizontal distance (see Equation S8 in the supplementary materials). For the best-fitting parameters,  $\omega$  was  $0.998 \pm 0.0004$  (M  $\pm$  SD),  $v_0$  was  $0.250 \pm 0.015^\circ/s$ , and  $w_m$  was  $0.506 \pm 0.061$ . The LCM predicts the deceleration tendency in which the PSE is a power function of the distance between two circles (see Equation S21 in the supplementary materials).  $\omega_s$  was  $0.940 \pm 0.007$ ,  $\sigma_{sm}$  was  $0.219 \pm 0.031$  s,  $v_0$  was  $0.088 \pm 0.016^\circ/s$ , and  $t_0$  was  $0.997 \pm 0.376$  s. The best-fitting parameters are presented in Supplementary Table 1 for each participant.

We further explored the individual differences in the Kappa effect based on the LCM. We defined  $\kappa = 1 - \omega_s = \frac{1}{(\sigma_{st}^2/\sigma_{sm}^2)+1}$  as an index of the

strength of the Kappa effect. A larger  $\kappa$  indicates a faster increase in the estimated time as the distance  $l$  between two circles increases (see Equation S15 in the supplementary materials).  $\sigma_{sm}$  is an index of the variability in time perception. We found a significantly positive correlation between  $\kappa$  and  $\sigma_{sm}$  ( $r = 0.719$ ,  $p < 0.05$ ; see Fig. 4D). These results indicate a close relationship between the variability of time perception and the strength of the Kappa effect.

We evaluated the goodness of fit of the model using the AIC index. A larger AIC indicates that the fitted model is less plausible. AIC  $\Delta$  was obtained by subtracting the AIC of the LCM from that of the classical model for each participant. The AIC  $\Delta$  ranged from 5.943 to 24.099. According to the levels of empirical support for the model ( $0 \leq \Delta \leq 2$  = substantial;  $4 \leq \Delta \leq 7$  = considerably less;  $\Delta > 10$  = essentially none; Burnham and Anderson, 2004), the LCM was superior to the classical model in terms of model fitting for all participants.

#### 4. General discussion

We used a time discrimination task to replicate the Kappa effect, in which the PSE increases along with the distance between two circles. We manipulated the vertical distance between circles and a central fixation, and produced evidence in Experiment 1 that the tendency to decelerate in the Kappa effect is not driven by the uncertainty of circle locations (see Fig. 2). We then manipulated the distances between sample circles

from 1° to 32° and compared fit levels between the classical model and the LCM in Experiment 2 (see Fig. 4). The AIC index provided quantitative evidence that the LCM fit the data better than the classical model.

We found that the main effect of vertical distance was not significant, which indicates that the spatial uncertainty of the circle locations does not influence the visual Kappa effect. Our results are inconsistent with the prediction of the slowness model that a given distance with a larger spatial uncertainty of stimuli locations will be perceived as shorter (Tong et al., 2016) and that a shorter distance will lead to a shorter duration perception (Chen et al., 2016; Goldreich, 2007). This contradiction may be due to the differences in spatial processing characteristics between visual and tactile modalities. The localization of touch on body parts is often inaccurate. In the cutaneous rabbit effect, for example, subjects can perceive a series of taps on the skin that does not exist (Geldard and Sherrick, 1972; Miyazaki et al., 2010). However, our visual localization was very precise. People can hit rapidly moving balls with exceptional precision (Land and McLeod, 2000). As predicted by the Bayesian observer model, tactile spatial processing is more inaccurate; thus, tactile processing can be easily interfered with by expectation (Tong et al., 2016). Therefore, the slowness model is not suitable for explaining the visual Kappa effect.

We replicated the deceleration tendency whereby the PSE increases more slowly with a longer distance than with a shorter distance, which is consistent with the prediction of the LCM rather than that of the classical model. The AIC results also showed that the LCM was superior to the classical model in data fitting. Chen et al. (2016) found the deceleration tendency in the 0.8-second condition, but a linear relation was found in the 1.2-second condition (see Supplementary Fig. 2). We fitted the models to the data drawn from Chen et al. (2016) and found that the LCM was not substantially different from the classical model in data fitting (see the supplementary materials for details). The difference between the two studies was due to the experimental paradigms. Previous studies have shown that motor response has an important influence on temporal performance in the time reproduction task; participants have been found to be able to estimate the time interval accurately but be unable to reproduce it accurately (Droit-Volet, 2010; Wearden, 2003). In the time discrimination task, participants need to estimate the standard and probe time intervals and decide which time interval is longer. The time discrimination task does not need to reproduce the time interval; thus, the influence of the motor response on the time estimation can be avoided. Therefore, the time discrimination task is more suitable for studying the deceleration tendency than the time reproduction task.

The key hypothesis of LCM is the logarithmic internal representation of time. The logarithmic internal time hypothesis was deduced from the scalar variability of time perception, in which the standard deviation of timing increased linearly as the time interval increased. The scalar variability is consistent with the Weber–Fechner law, which determines a logarithmic internal representation of time (Brannon et al., 2008; Gibbon, 1977; Gibbon et al., 1984; Wearden, 1999). However, several studies have reported that time estimation follows Stevens' power law (Bobko et al., 1977; Eisler, 1976; Grondin and Laflamme, 2015). Studies have revealed that the Bayesian model provides a direct link between Weber–Fechner's law and Stevens' power law (Petzschner et al., 2015; Petzschner and Glasauer, 2011). Our Bayesian model shows that the internal time is a logarithmic function of physical time and physical distance (Equation S15), which follows the Weber–Fechner law. A motor response  $t_e$ , which is the estimated time in the time reproduction task or verbal estimation task, is a power function of physical time and physical distance (Equation S17), and the PSE is a power function of physical distance (Equation S21), which follows Stevens' power law. Therefore, our study provides evidence that the deceleration tendency is driven by the Weber–Fechner law.

The speed prior is the basic hypothesis of the three Bayesian models. The slowness model assumes a low speed prior to the movement of objects at a low speed with a mean of zero (Freeman et al., 2010; Stocker and Simoncelli, 2006; Weiss et al., 2002). The classical model and LCM

both assume a constant speed prior to objects moving at a constant speed (Jones and Huang, 1982). We found that the estimated constant speed of the classical model (0.25°/s) is close to the absolute threshold of speed for older people with a mean age of 62 (0.12°/s), while the estimated constant speed of the LCM (0.09°/s) is equal to the absolute threshold of speed for younger people with a mean age of 23 (Snowden and Kavanagh, 2006). We refitted the classical model and the LCM to the data in Chen et al. (2016) using the bootstrap method. The constant speed was approximately 0.2°/s for the classical model and approximately 0.7°/s for the LCM (see supplementary materials for details). Although Chen et al. (2016) did not use the bootstrap method, they also reported that the constant speed was approximately 0.2°/s for the classical model. Thus, our results confirmed the previous finding that the constant speed was slow.

We defined  $\kappa$  as an index of the strength of the Kappa effect and found that  $\kappa$  positively correlated with the variability of time perception. To the best of our knowledge, this is the first report of individual differences in the Kappa effect, whereby individuals with a more precise time perception have a weaker Kappa effect. This result is consistent with the widely accepted notion of Bayesian theory that humans' reliance on prior knowledge increases as the uncertainty of a task increases (Körding, 2007; Körding et al., 2004; Pouget et al., 2013; Stocker and Simoncelli, 2006). Studies have proposed that spatiotemporal interferences are especially correlated to depend on the variability of the perceived dimensions (Cai et al., 2018; Cai and Connell, 2015); however, these studies provide only qualitative evidence (interference vs. no interference). Our study provides not only a theoretical function between the strength of the Kappa effect and the variability of time perception ( $\kappa = \frac{1}{(\frac{\sigma_{\kappa}^2}{\sigma_{\kappa m}^2} + 1)}$ ) but quantitative empirical evidence as well (see Fig. 4D).

## 5. Conclusions

We performed two experiments to determine why spatiotemporal interference is accompanied by a deceleration tendency. In Experiment 1, we found that the uncertainty of stimuli locations did not modulate the estimated time, which suggests that the slowness model, originating from tactile neural activities, is not suitable for explaining the visual Kappa effect. In Experiment 2, we found that the Bayesian model on logarithmic scales made better behavioral predictions than the linear model and provided a theoretical framework with which to integrate the logarithmic time representation with power time estimation. The estimated constant speed was close to the absolute threshold of speed, which confirms the previous finding that the Kappa effect is driven by slow speeds. Based on the logarithmic Bayesian model,  $\kappa$  was defined as an index of the strength of the Kappa effect and was found to be positively correlated with the variability of time perception. Our findings suggest that the deceleration tendency in spatiotemporal interferences is driven by the Weber–Fechner law. The unifying Bayesian framework helps explain the Kappa effect and may be applied in the field of time perception and other types of cross-dimensional interference with the appropriate assumptions in future work.

## CRedit authorship contribution statement

**Yoguo Chen:** Conceptualization, Methodology, Formal analysis, Writing - original draft. **Chunhua Peng:** Investigation, Data curation. **Andrew Avitt:** Writing - review & editing.

## Acknowledgements

This study was supported by Humanities and Social Science Youth Foundation of Ministry of Education of China (Grant No. 19YJC190002) and Fundamental Research Funds for the Central Universities (Grant No. SWU1909444).

## Appendix A. Supplementary data

Supplementary data to this article can be found online at <https://doi.org/10.1016/j.visres.2021.06.005>.

## References

- Akaike, H. (1974). A new look at the statistical model identification. *IEEE Transactions on Automatic Control*, 19(6), 716–723. <https://doi.org/10.1109/TAC.1974.1100705>.
- Bobko, D. J., Thompson, J. G., & Schiffman, H. R. (1977). The perception of brief temporal intervals: Power functions for auditory and visual stimulus intervals. *Perception*, 6(6), 703–709. <https://doi.org/10.1068/p060703>.
- Brainard, D. H. (1997). The psychophysics toolbox. *Spatial Vision*, 10(4), 433–436. <https://doi.org/10.1163/156856897X00357>.
- Brannon, E. M., Libertus, M. E., Meck, W. H., & Woldorff, M. G. (2008). Electrophysiological measures of time processing in infant and adult brains: Weber's law holds. *Journal of Cognitive Neuroscience*, 20(2), 193–203. <https://doi.org/10.1162/jocn.2008.20016>.
- Burnham, K. P., & Anderson, D. R. (2004). *Model Selection and Multimodel Inference: A Practical Information-Theoretic Approach* (2nd ed.). Springer.
- Burr, D., Tozzi, A., & Morrone, M. C. (2007). Neural mechanisms for timing visual events are spatially selective in real-world coordinates. *Nature Neuroscience*, 10(4), 423–425.
- Burr, D., Banks, M. S., & Morrone, M. C. (2009). Auditory dominance over vision in the perception of interval duration. *Experimental Brain Research*, 198(1), 49–57. <https://doi.org/10.1007/s00221-009-1933-z>.
- Cai, Z. G., & Connell, L. (2015). Space–time interdependence: Evidence against asymmetric mapping between time and space. *Cognition*, 136, 268–281. <https://doi.org/10.1016/j.cognition.2014.11.039>.
- Cai, Z. G., Wang, R., Shen, M., & Speekenbrink, M. (2018). Cross-dimensional magnitude interactions arise from memory interference. *Cognitive Psychology*, 106, 21–42. <https://doi.org/10.1016/j.cogpsych.2018.08.001>.
- Casasanto, D., & Boroditsky, L. (2008). Time in the mind: Using space to think about time. *Cognition*, 106(2), 579–593. <https://doi.org/10.1016/j.cognition.2007.03.004>.
- Chang, C.-J., & Jazayeri, M. (2018). Integration of speed and time for estimating time to contact. *Proceedings of the National Academy of Sciences of the United States of America*, 115(12), E2879–E2887. <https://doi.org/10.1073/pnas.1713316115>.
- Chen, Y., Zhang, B., Kording, K. P., & Luo, W. (2016). Speed constancy or only slowness: What drives the Kappa effect. *e0154013 PLoS ONE*, 11(4). <https://doi.org/10.1371/journal.pone.0154013>.
- Cohen, J. (1988). *Statistical Power Analysis for the Behavioral Sciences* (2nd ed.). Erlbaum.
- Cohen, J., Hansel, C. E. M., & Sylvester, J. D. (1955). Interdependence in judgments of space, time and movement. *Acta Psychologica*, 11, 360–372. [https://doi.org/10.1016/S0001-6918\(55\)80098-4](https://doi.org/10.1016/S0001-6918(55)80098-4).
- Cohen, J., Hansel, C. E., & Sylvester, J. D. (1953). A new phenomenon in time judgment. *Nature*, 172(4385), 901.
- Collyer, C. E. (1976). The induced asynchrony effect: Its role in visual judgments of temporal order and its relation to other dynamic perceptual phenomena. *Perception & Psychophysics*, 19(1), 47–54.
- Dehaene, S. (2003). The neural basis of the Weber-Fechner law: A logarithmic mental number line. *Trends in Cognitive Sciences*, 7(4), 145–147. [https://doi.org/10.1016/S1364-6613\(03\)00055-X](https://doi.org/10.1016/S1364-6613(03)00055-X).
- Dehaene, S., Izard, V., Spelke, E., & Pica, P. (2008). Log or linear? Distinct intuitions of the number scale in Western and Amazonian indigene cultures. *Science*, 320(5880), 1217–1220. <https://doi.org/10.1126/science.1156540>.
- Droit-Volet, S. (2010). Stop using time reproduction tasks in a comparative perspective without further analyses of the role of the motor response: The example of children. *European Journal of Cognitive Psychology*, 22(1), 130–148. <https://doi.org/10.1080/09541440902738900>.
- Durgin, F. H., Akagi, M., Gallistel, C. R., & Haiken, W. (2009). The precision of locomotor odometry in humans. *Experimental Brain Research*, 193(3), 429–436. <https://doi.org/10.1007/s00221-008-1640-1>.
- Eisler, H. (1976). Experiments on subjective duration 1868–1975: A collection of power function exponents. *Psychological Bulletin*, 83(6), 1154–1171.
- Fechner, G. T. (1860). *Elemente der Psychophysik*. Breitkopf & Härtel.
- Freeman, T. C., Champion, R. A., & Warren, P. A. (2010). A Bayesian model of perceived head-centered velocity during smooth pursuit eye movement. *Current Biology*, 20(8), 757–762. <https://doi.org/10.1016/j.cub.2010.02.059>.
- Geldard, F. A., & Sherrick, C. E. (1972). The cutaneous “rabbit”: A perceptual illusion. *Science*, 178(4057), 178–179. <https://doi.org/10.1126/science.178.4057.178>.
- Gibbon, J. (1977). Scalar expectancy theory and Weber's law in animal timing. *Psychological Review*, 84(3), 279–325. <https://doi.org/10.1037/0033-295X.84.3.279>.
- Gibbon, J., & Church, R. M. (1981). Time left: Linear versus logarithmic subjective time. *Journal of Experimental Psychology: Animal Behavior Processes*, 7(2), 87–107.
- Gibbon, J., Church, R. M., & Meck, W. (1984). Scalar timing in memory. In J. Gibbon, & L. Allan (Eds.), *Annals of the New York Academy of Sciences: Timing and time perception* (pp. 52–77). New York Academy of Sciences.
- Goldreich, D. (2007). A Bayesian perceptual model replicates the cutaneous rabbit and other tactile spatiotemporal illusions. *e333 PLoS ONE*, 2(3). <https://doi.org/10.1371/journal.pone.0000333>.
- Goldreich, D., & Tong, J. (2013). Prediction, postdiction, and perceptual length contraction: A Bayesian low-speed prior captures the cutaneous rabbit and related illusions. *Frontiers in Psychology*, 4, 221. <https://doi.org/10.3389/fpsyg.2013.00221>.
- Greenhouse, S. W., & Geisser, S. (1959). On methods in the analysis of profile data. *Psychometrika*, 24(2), 95–112. <https://doi.org/10.1007/BF02289823>.
- Grondin, S., & Laflamme, V. (2015). Stevens's law for time: A direct comparison of prospective and retrospective judgments. *Attention Perception & Psychophysics*, 77(4), 1044–1051. <https://doi.org/10.3758/s13414-015-0914-5>.
- Huang, Y. L., & Jones, B. (1982). On the interdependence of temporal and spatial judgments. *Perception & Psychophysics*, 32(1), 7–14.
- Jogan, M., & Stocker, A. A. (2015). Signal integration in human visual speed perception. *Journal of Neuroscience*, 35(25), 9381–9390. <https://doi.org/10.1523/JNEUROSCI.4801-14.2015>.
- Jones, B., & Huang, Y. L. (1982). Space-time dependencies in psychophysical judgment of extent and duration: Algebraic models of the tau and kappa effects. *Psychological Bulletin*, 91(1), 128–142. <https://doi.org/10.1037/0033-2909.91.1.128>.
- Klein, S., & Levi, D. (1987). Position sense of the peripheral retina. *Journal of the Optical Society of America*, 4(8), 1543–1553. <https://doi.org/10.1364/josaa.4.001543>.
- Körding, K. P. (2007). Decision theory: What “should” the nervous system do? *Science*, 318(5850), 606–610. <https://doi.org/10.1126/science.1142998>.
- Körding, K. P., Ku, S.-p., & Wolpert, D. M. (2004). Bayesian integration in force estimation. *Journal of Neurophysiology*, 92(5), 3161–3165.
- Lakshminarasimhan, K. J., Petsalis, M., Park, H., DeAngelis, G. C., Pitkow, X., & Angelaki, D. E. (2018). A dynamic Bayesian observer model reveals origins of bias in visual path integration. *Neuron*, 99(1), 194–206.e5. <https://doi.org/10.1016/j.neuron.2018.05.040>.
- Land, M. F., & McLeod, P. (2000). From eye movements to actions: How batsmen hit the ball. *Nature Neuroscience*, 3(12), 1340–1345. <https://doi.org/10.1038/81887>.
- Levi, D., & Klein, S. (1990). The role of separation and eccentricity in encoding position. *Vision Research*, 30(4), 557–585. [https://doi.org/10.1016/0042-6989\(90\)90068-V](https://doi.org/10.1016/0042-6989(90)90068-V).
- Levi, D. M., Klein, S. A., & Yap, Y. L. (1988). “Weber's law” for position: Unconfounding the role of separation and eccentricity. *Vision Research*, 28(5), 597–603. [https://doi.org/10.1016/0042-6989\(88\)90109-5](https://doi.org/10.1016/0042-6989(88)90109-5).
- Levine, T. R., & Hullett, C. R. (2002). Eta squared, partial eta squared, and misreporting of effect size in communication research. *Human Communication Research*, 28(4), 612–625. <https://doi.org/10.1111/j.1468-2958.2002.tb00828.x>.
- Malone, H. E., Nicholl, H., & Coyne, I. (2016). Fundamentals of estimating sample size. *Nurse Res*, 23(5), 21–25. <https://doi.org/10.7748/nr.23.5.21.s5>.
- Masuda, T., Kimura, A., Dan, I., & Wada, Y. (2011). Effects of environmental context on temporal perception bias in apparent motion. *Vision Research*, 51(15), 1728–1740. <https://doi.org/10.1016/j.visres.2011.05.016>.
- Meese, T. S. (1995). Using the standard staircase to measure the point of subjective equality: A guide based on computer simulations. *Perception & Psychophysics*, 57(3), 267–281.
- Miyazaki, M., Hirashima, M., & Nozaki, D. (2010). The “Cutaneous Rabbit” hopping out of the body. *Journal of Neuroscience*, 30(5), 1856–1860. <https://doi.org/10.1523/Jneurosci.3887-09.2010>.
- Oliveri, M., Koch, G., & Caltagirone, C. (2009). Spatial-temporal interactions in the human brain. *Experimental Brain Research*, 195(4), 489–497. <https://doi.org/10.1007/s00221-009-1834-1>.
- Petzschner, F. H., & Glasauer, S. (2011). Iterative Bayesian estimation as an Explanation for range and regression effects: A study on human path Integration. *Journal of Neuroscience*, 31(47), 17220–17229. <https://doi.org/10.1523/Jneurosci.2028-11.2011>.
- Petzschner, F. H., Glasauer, S., & Stephan, K. E. (2015). A Bayesian perspective on magnitude estimation. *Trends in Cognitive Sciences*, 19(5), 285–293. <https://doi.org/10.1016/j.tics.2015.03.002>.
- Pöppel, E. (1997). A hierarchical model of temporal perception. *Trends in Cognitive Sciences*, 1(2), 56–61. [https://doi.org/10.1016/S1364-6613\(97\)01008-5](https://doi.org/10.1016/S1364-6613(97)01008-5).
- Pouget, A., Beck, J. M., Ma, W. J., & Latham, P. E. (2013). Probabilistic brains: Knowns and unknowns. *Nature Neuroscience*, 16(9), 1170–1178. <https://doi.org/10.1038/nn.3495>.
- Price-Williams, D. R. (1954). The Kappa effect. *Nature*, 173(4399), 363–364. <https://doi.org/10.1038/173363a0>.
- Snowden, R. J., & Kavanagh, E. (2006). Motion perception in the ageing visual system: Minimum motion, motion coherence, and speed discrimination thresholds. *Perception*, 35(1), 9–24. <https://doi.org/10.1068/p5399>.
- Stocker, A. A., & Simoncelli, E. P. (2006). Noise characteristics and prior expectations in human visual speed perception. *Nature Neuroscience*, 9(4), 468–470. <https://doi.org/10.1038/nn1669>.
- Szelag, E., Kowalska, J., Rymarczyk, K., & Poppel, E. (2002). Duration processing in children as determined by time reproduction: Implications for a few seconds temporal window. *Acta Psychologica*, 110(1), 1–19. [https://doi.org/10.1016/S0001-6918\(01\)00067-1](https://doi.org/10.1016/S0001-6918(01)00067-1).
- Tong, J., Ngo, V., & Goldreich, D. (2016). Tactile length contraction as Bayesian inference. *Journal of Neurophysiology*, 116(2), 369–379. <https://doi.org/10.1152/jn.0029.2016>.
- Ulbrich, P., Churan, J., Fink, M., & Wittmann, M. (2007). Temporal reproduction: Further evidence for two processes. *Acta Psychologica*, 125(1), 51–65. <https://doi.org/10.1016/j.actpsy.2006.06.004>.
- Walsh, V. (2003). A theory of magnitude: Common cortical metrics of time, space and quantity. *Trends in Cognitive Sciences*, 7(11), 483–488. <https://doi.org/10.1016/j.tics.2003.09.002>.
- Waugh, S. J., & Levi, D. M. (1993). Visibility and vernier acuity for separated targets. *Vision Research*, 33(4), 539–552. [https://doi.org/10.1016/0042-6989\(93\)90257-W](https://doi.org/10.1016/0042-6989(93)90257-W).

- Wearden, J. (2003). Applying the scalar timing model to human time psychology: Progress and challenges. In H. Helfrich (Ed.), *Time and mind II: Information processing perspectives* (pp. 21–39). Hogrefe & Huber Publishers.
- Wearden, J. H. (1999). “Beyond the fields we know...”: Exploring and developing scalar timing theory. *Behavioural Processes*, 45(1–3), 3–21.
- Weiss, Y., Simoncelli, E. P., & Adelson, E. H. (2002). Motion illusions as optimal percepts. *Nature Neuroscience*, 5(6), 598–604. <https://doi.org/10.1038/Nn858>.
- Wickens, T. D. (2001). *Elementary signal detection theory*. Oxford University Press.
- Wilson, H. R. (1991). Pattern discrimination, visual filters, and spatial sampling irregularity. In M. Landy, & J. A. Movshon (Eds.), *Computational Models of Visual Processing* (pp. 153–168). Cambridge, Mass.: MIT Press.
- World Medical Association. (2013). WMA declaration of Helsinki—Ethical principles for medical research involving human subjects. <<http://www.wma.net/en/30publications/10policies/b3/index.html>>.